Vol 10 No 7, July 2001
1009-1963/2001/10(07)/0587-07

Chinese Physics

© 2001 Chin. Phys. Soc.
and IOP Publishing Ltd

SOME PROGRESS IN THE LATTICE BOLTZMANN MODEL*

Feng Shi-de(冯士德)[a], Tsutahara Michihisa[b], and Ji Zhong-zhen(季仲贞)[a]

[a] *Laboratory of Numerical Modelling for Atmospheric Sciences and Geophysical Fluid Dynamics, Institute of Atmospheric Physics, Chinese Academy of Sciences, Beijing* 100029, *China*

[b] *Division of Industrial Science, Graduate School of Technology and Science, Kobe University, Japan*

(Received 16 January 2001)

A lattice Boltzmann equation model has been developed by using the equilibrium distribution function of the Maxwell–Boltzmann-like form, which is third order in fluid velocity u_α. The criteria of energy conservation between the macroscopic physical quantities and the microscopic particles are introduced into the model, thus the thermal hydrodynamic equations containing the effect of buoyancy force can be recovered in terms of the Taylor and Chapman–Enskog asymptotic expansion methods. The two-dimensional thermal convection phenomena in a square cavity and between two concentric cylinders have been calculated by implementing a heat flux boundary condition. Both numerical results are in good agreement with the conventional numerical results.

Keywords: lattice Boltzmann equation model, hydrodynamic equations, thermal convection
PACC: 0340, 0340G, 0340K

I. INTRODUCTION

Macroscopic physical fluids consist of discrete particles on a microscopic level, therefore the macroscopic behaviour of fluid flow can be simulated by microscopic mechanics methods. One of these is the lattice Boltzmann equation model (LBE). Because the LBE has been developed based on the lattice gas automaton model (LGA), it overcomes two drawbacks of the LGA model, i.e. the non-Galilean invariance property and the unphysical equations of state,[1] so that it can be approximately reduced to the Navier–Stokes equations at macroscopic level. It has been proven that the lattice Boltzmann equation model is valid for the numerical simulation of a fluid flow in theory. However, the simulation of the heat diffusion system by the thermal LBE model[5] has not achieved success as a result of severe numerical instability. Though the Rayleigh–Benard convection is successfully simulated to a certain degree in Ref.[6], the model is not a real thermal LBE model. In fact, it employs a two-component system: component 1 represents the motion of the fluid and component 2 simulates a passive temperature field. Obviously such a model cannot strictly satisfy the equation of energy conservation. To get rid of the defect, we have developed a LBE model for a multiple-particle system based on previous work.[4−7] The LBE model strictly satisfies the equation of energy conservation. In the LBE model, the internal energy of fluid per unit mass determined by the particle speed is in agreement with the principle of statistical physics, and the local equilibrium distribution of the Maxwell–Boltzmann-like form is third order in the fluid component velocity u_α. In order to simulate the phenomena of fluid flow in the gravity field, the effect of buoyancy force has been introduced into the model by adding a fixed amount of momentum at each node in terms of Ref.[3]. Both thermal convection phenomena in two dimensions in the numerical experiment have been successfully simulated by using the $D2Q9$ LBE model.

II. NUMERICAL MODEL

The fictitious microscopic particle world and the macroscopic fluid world can be related to the Boltzmann equation through the medium of a velocity distribution function. In general, the traditional local equilibrium distribution can be written as a truncated power series in macroscopic fluid flow velocity u_α,[9] which is second order in u_α. The local equilibrium distribution of the Maxwell–Boltzmann-like form is

$$f_{ki}^{(0)} = A_k \rho_k^* \exp[E_k(e_{ki\alpha} - v_\alpha)^2]. \qquad (1)$$

The local equilibrium distribution may be rewritten in non-dimensional form by introducing the characteristic particle speed c_0 and a reference density ρ_∞, that

*Project supported by the National Natural Science Foundation of China (Grant Nos. 49823002, 7-200053, 4-200060 and 8-1502) and by the National Key Planning Development Project for Basic Research (Grant No. G1999032801).

is

$$
\begin{aligned}
& f_{ki}^{\mathrm{eq}} = A_k \rho_k \exp[E_k (c_{ki\alpha} - u_\alpha)^2], \qquad (2)\\
& k = 1, 2, \cdots, n,\\
& i = 0, 1, \cdots, b,\\
& c_{ki\alpha} = e_{ki\alpha}/c_0,\\
& u_\alpha = v_\alpha / c_0,\\
& \rho_k = \rho_k^* / \rho_\infty,
\end{aligned}
$$

where ρ_k is the fluid density of the kth component, α represents the Cartesian coordinates, and the weights A_k and the factors E_k are determined by the conservation of mass, momentum and energy. For an equilibrium state, the local equilibrium distribution f_{ki}^{eq} is defined as an average of the particle number in a population associated with the link i of a node at position r_α, time t and moving speed $c_{ki\alpha}$, and it depends only on the local macroscopic physical quantities, i.e. the fluid density ρ_k and velocity u_α. The local equilibrium distribution f_{ki}^{eq} (2) is expanded in terms of the Taylor series about u_α=0 accurate to third order in u_α:

$$
\begin{aligned}
f_{ki}^{\mathrm{eq}} =& W_k \rho_k (1 - 2E_k c_{ki\alpha} u_\alpha + 2K_k^2 c_{ki\alpha} c_{ki\beta} u_\alpha u_\beta + E_k u^2\\
& - 2E_k^2 c_{ki\alpha} u_\alpha u^2 - \frac{4}{3} E_k^3 c_{ki\alpha} c_{ki\beta} c_{ki\chi} u_\alpha u_\beta u_\chi), \quad (3)\\
W_k =& A_k \mathrm{e}^{E_k c_k^2},
\end{aligned}
$$

where all particle speeds $c_{ki\alpha}$ have the same norm c_k, and β and χ represent Cartesian coordinates.

The conservation criteria between the macroscopic physical quantities and microscopic particle populations are defined as,[4] mass criterion:

$$
\rho = \sum_k \sum_i f_{ki}, \qquad (4)
$$

momentum criterion:

$$
\rho u_\alpha = \sum_k \sum_i f_{ki} c_{ki\alpha}, \qquad (5)
$$

energy criterion:

$$
\begin{aligned}
& \frac{1}{2} \rho u^2 + \rho e = \frac{1}{2} \sum_k \sum_i f_{ki} c_k^2, \qquad (6)\\
& \rho e = \sum_k \rho_k e_k,
\end{aligned}
$$

where e and e_k are the internal energy of fluid and its kth component per unit mass, and e_k is a constant. In order to recover accurately the Eulerian and Navier–Stokes equations, the momentum flux must be defined as

$$
P \delta_{\alpha\beta} + \rho u_\alpha u_\beta = \sum_k \sum_i f_{ki}^{\mathrm{eq}} c_{ki\alpha} c_{ki\beta}, \qquad (7)
$$

$$
\delta_{\alpha\beta} = \begin{cases} 1, & \alpha = \beta \\ 0, & \alpha \neq \beta \end{cases},
$$

where P is the pressure.

In order to find the weights W_k and the factors E_k, we introduce the important properties for the symmetries of the tensors. For orthogonal lattices of face-centred-cubic as shown in Fig.1, the isotropic tensors $E^{(n)}$ in D-dimensional space can take the form:

$$
\begin{cases}
E^{(2n+1)} = 0,\\
E^{(2n)} = \sum_{i=1}^{b} (c_{ki\alpha} \cdots c_{ki\alpha})^{2n} = \dfrac{b}{D} c_k^{2n},
\end{cases} \qquad (8)
$$

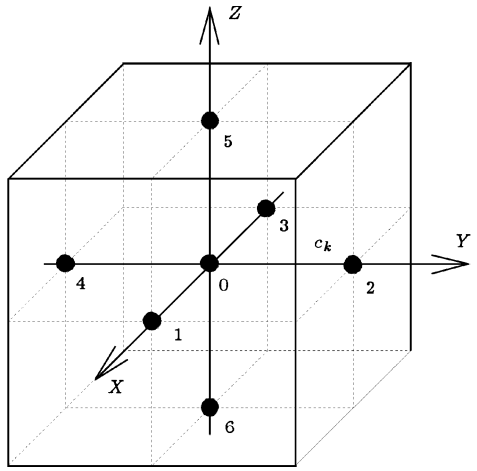


Fig.1. An orthogonal lattice of face-centred-cubic. All particle speeds have the same norm c_k.

for two-dimensional space $D = 2$, $b = 4$, and for three-dimensional space $D = 3$, $b = 6$. If the lattice is face-centred-cubic, as shown in Fig.2, the isotropic tensors $E^{(n)}$ in D-dimensional space can take the form:

$$
\begin{cases}
E^{(2n+1)} = 0,\\
E^{(2n)} = \sum_{i=1}^{b} (c_{ki\alpha} \cdots c_{ki\alpha})^{2n} = \dfrac{b}{2^{(n-1)} D} c_k^{2n},
\end{cases} \qquad (9)
$$

for two-dimensional space $D = 2$, $b = 4$, and for three-dimensional space $D = 3$, $b = 12$. If the lattice is the cubic lattice, as shown in Fig.3, the isotropic tensors $E^{(n)}$ in D-dimensional space can take the form:

$$\begin{cases} E^{(2n+1)} = 0 \\ E^{(2n)} = \sum_{i=1}^{b} (c_{ki\alpha} \cdots c_{ki\alpha})^{2n} = \dfrac{b}{D^n} c_k^{2n} \end{cases} . \quad (10)$$

Equation (10) is only valid for the three-dimensional space $D = 3$, $b = 8$.

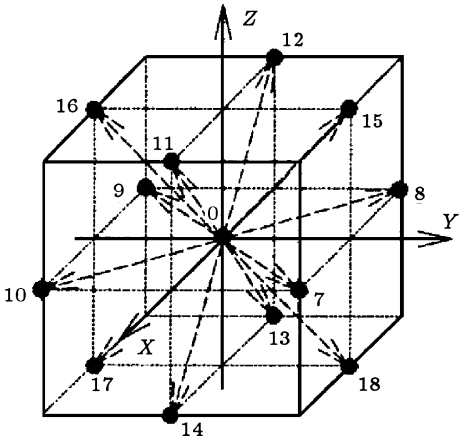


Fig.2. A symmetric-orthogonal cubic lattice. All particle speeds have the same norm $\sqrt{2}\ c_k$.

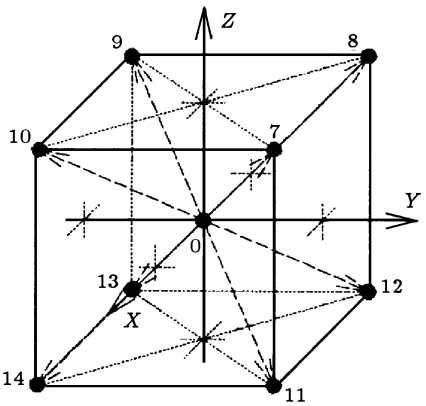


Fig.3. A symmetry cubic lattice. All particle speeds have the same norm $\sqrt{3}\ c_k$.

For the hexagonal lattice, Ref.[2] has already given the properties of the isotropic tensors in two-dimensional space.

In terms of the Chapman–Enskog asymptotic expansion method, the velocity distribution function f_{ki} differs only slightly from their local equilibrium distribution function values f_{ki}^{eq}.[2] In other words, the velocity distribution function f_{ki} can be regarded as a composition of the local equilibrium distribution f_{ki}^{eq} and the non-equilibrium components f_{ki}^{neq}, that is

$$f_{ki} = f_{ki}^{\mathrm{eq}} + f_{ki}^{\mathrm{neq}}. \quad (11)$$

The non-equilibrium component f_{ki}^{neq} should not contribute to the local values of density, mean momentum and energy, and it satisfies the following criteria[1]

$$f_{ki}^{\mathrm{neq}} = O(\varepsilon), \quad (12)$$

$$\partial^n f_{ki}^{\mathrm{neq}} = O(\varepsilon^{n+1}), \quad (13)$$

$$\sum_k \sum_i f_{ki}^{\mathrm{neq}} = 0, \quad (14)$$

$$\sum_k \sum_i f_{ki}^{\mathrm{neq}} c_{ki\alpha} = 0, \quad (15)$$

$$\sum_k \sum_i f_{ki}^{\mathrm{neq}} c_k^2 = 0. \quad (16)$$

In terms of the above conservation criteria from (4) to (7), the properties of the isotropic tensors and the Chapman–Enskog asymptotic expansion, the weights W_k and the factors E_k can be found, as shown in table 1.

Ⅲ. HYDRODYNAMIC EQUATIONS

In order to further verify the validity of the LBE model for the numerical simulation of fluid flow in theory, a recovery procedure of the hydrodynamic equations can usually be employed using the BGK equation.[5] To simulate the thermal convection phe-

Table 1. Sample values for $DdQb$ LBE models with D-dimensional space and b particle speeds.

Models	E_k	W_0	W_1	W_2	W_3	P	c_k^2
$D1Q3$	$-\dfrac{2}{2c_k^2}$	$\dfrac{3-D}{3}$	$\dfrac{D}{3b}$				
$D2Q7$	$-\dfrac{D}{4e_k}$	$\dfrac{D}{D+2}$	$\dfrac{D}{b(D+2)}$			$\dfrac{2}{D}\rho e$	$\dfrac{2e_k(2+D)}{D}$
$D2Q9$	$-\dfrac{D}{4e_k}$	$\dfrac{18-5D}{18}$	$\dfrac{2D}{9b_1}$	$\dfrac{D}{18b_2}$	$b_1 = 4$ $b_2 = 4$	$\dfrac{2}{D}\rho e$	$\dfrac{6e_k}{D}$
$D3Q15$	$-\dfrac{(6+D)D}{36e_k}$	$1 - \dfrac{D(18+D)}{(6+D)^2}$	$\dfrac{18D}{b_1(6+D)^2}$	$b_1 = 6$ $b_3 = 8$	$\dfrac{D^2}{b_3(6+D)^2}$	$\dfrac{2}{D}\rho e$	$\dfrac{6e_k}{D}$
$D3Q19$	$-\dfrac{D}{4e_k}$	$\dfrac{9-2D}{9}$	$\dfrac{D}{9b_1}$	$\dfrac{D}{9b_2}$	$b_1 = 6$ $b_2 = 12$	$\dfrac{2}{D}\rho e$	$\dfrac{6e_k}{D}$

nomena, we have to consider a lattice BGK equation including an external force. The effect of external forces, such as gravity, may be represented by adding a fixed external force term $\boldsymbol{F}_{ki}$ in each node[3] as shown in Figs.4 and 5; it can also be called the effect of buoyancy force in a buoyancy field. In terms of the corresponding forcing scheme, the lattice BGK equation is given by:

$$\begin{aligned} &f_{ki}(r_\alpha + c_{ki\alpha}\delta t, t+\delta t) - f_{ki}(r_\alpha, t) \\ =&\boldsymbol{F}_{ki}\cdot\boldsymbol{K}_k\boldsymbol{k}_{\alpha i} - \Omega_{ki}, \end{aligned} \tag{17}$$

$$\boldsymbol{F}_{ki} = \delta t\eta\frac{f_{ki}}{c_{ki\alpha}}\boldsymbol{g},$$

$$\Omega_{ki} = \frac{1}{\tau}[f_{ki}(r_\alpha, t) - f_{ki}^{\mathrm{eq}}(r_\alpha, t)],$$

where δt is a discrete timescale, $\boldsymbol{g}$ is the gravity acceleration, $\boldsymbol{k}_\alpha$ is a unit vertical vector in the α-direction, η is a perturbation strength parameter, Ω_{ki} is a collision operator, and τ is a dimensionless relaxation time coefficient. The difference between the velocity function in the left-hand side of Eq.(17) and Ω_{ki} can be found to be first order in ε by using the Taylor and the Chapman–Enskog asymptotic expansion methods. Therefore, the effect of buoyancy force $\boldsymbol{F}_{ki}$ must be also first order in ε. The perturbation strength parameter η should satisfy $|\eta| \ll 1$, since $\boldsymbol{F}_{ki}$ is first order in ε. The perturbation strength parameter η in a buoyancy field is determined by the Grashof number Gr. In addition, the particle populations are subject to the action of the buoyancy force. Thus, the product of η and f_{ki} may be regarded as a perturbation value of distribution function, that is

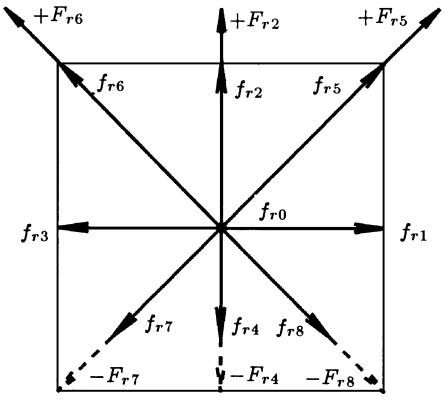


Fig.4. The effect of buoyancy force for hot particles in the vertical direction.

$$\eta f_{ki} = f_{ki} - f_{0ki}, \tag{18}$$

where f_{0ki} is a reference distribution function for a state of hydrostatic equilibrium. If $\eta > 0$, the particle tends to lift as shown in Fig.4. If $\eta < 0$, the particle tends to sink as shown in Fig.5.

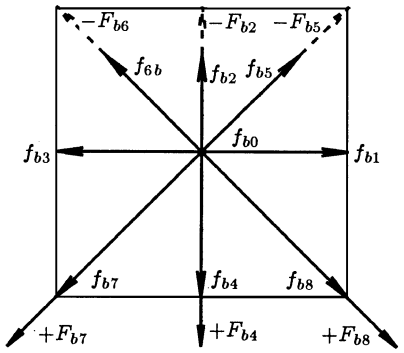


Fig.5. The effect of buoyancy force for cold particles in the vertical direction.

The first term $f_{ki}(r_\alpha + c_{ki\alpha}\delta t, t+\delta t)$ in Eq.(17) is expanded in terms of the Taylor series and is accurate to first and second order in δt, respectively. We obtain

$$\frac{\partial f_{ki}}{\partial t} + c_{ki\alpha}\frac{\partial f_{ki}}{\partial r_\alpha} = \frac{\boldsymbol{F}_{ki}\cdot\boldsymbol{K}_\alpha}{\delta t}\frac{1}{\tau\delta t}[f_{ki} - f_{ki}^{\mathrm{eq}}], \tag{19}$$

$$\begin{aligned} &\frac{\partial f_{ki}}{\partial t} + c_{ki\alpha}\frac{\partial f_{ki}}{\partial r_\alpha} + \frac{\delta t}{2}c_{ki\alpha}c_{ki\beta}\frac{\partial^2 f_{ki}}{\partial r_\alpha \partial r_\beta} \\ &+ \delta t c_{ki\alpha}\frac{\partial^2 f_{ik}}{\partial t\partial r_\alpha} + \frac{\delta t}{2}\frac{\partial^2 f_{ki}}{\partial t^2} \\ =&\frac{\boldsymbol{F}_{ki}\cdot\boldsymbol{K}_\alpha}{\delta t} - \frac{1}{\tau\delta t}[f_{ki} - f_{ki}^{\mathrm{eq}}]. \end{aligned} \tag{20}$$

Substituting Eqs.(11), (12) and (13) into Eq.(19) and (20), respectively, we can obtain the two following equations which are first and second order in ε, respectively:

$$\frac{\partial f_{ki}^{\mathrm{eq}}}{\partial t} + c_{ki\alpha}\frac{\partial f_{ki}^{\mathrm{eq}}}{\partial r_\alpha} = \frac{\boldsymbol{F}_{ki}\cdot\boldsymbol{K}_\alpha}{\delta t} - \frac{1}{\tau\delta t}f_{ki}^{\mathrm{neq}}, \tag{21}$$

$$\begin{aligned} &\frac{\partial f_{ki}^{\mathrm{eq}}}{\partial t} + c_{ki\alpha}\frac{\partial f_{ki}^{\mathrm{eq}}}{\partial r_\alpha} + \left(1 - \frac{1}{2\tau}\right) \\ &\cdot\left(\frac{\partial f_{ki}^{\mathrm{neq}}}{\partial t} + c_{ki\alpha}\frac{\partial f_{ki}^{\mathrm{neq}}}{\partial r_\alpha}\right) = \frac{F_{ki}}{\delta t} - \frac{1}{\tau\delta t}f_{ki}^{\mathrm{neq}}. \end{aligned} \tag{22}$$

Summing Eq.(21) and considering Eqs.(4), (5) and (14), we obtain the continuity equation

$$\frac{\partial\rho}{\partial t} + \nabla\cdot(\rho\boldsymbol{u}) = 0. \tag{23}$$

Summing the moment of Eq.(22) with the particle speed $c_{ki\alpha}$ and considering Eqs.(5), (7), (15), (18) and (21), and leaving out third order in ε, we can obtain the incompressible momentum equation for the low

Mach constraint

$$\frac{\partial(\rho \boldsymbol{u})}{\partial t}+\boldsymbol{u}\cdot\nabla(\rho\boldsymbol{u})=-\nabla P+\eta\rho g\boldsymbol{k}+\nu\nabla^2(\rho\boldsymbol{u}), \quad (24)$$

$$P=\frac{2}{D}\rho e,$$

$$\nu=\frac{2e\delta t}{D}\left(\tau-\frac{1}{2}\right),$$

where ν is the kinematic viscosity, $\eta\rho$ is a perturbation value of the density ρ. If $\eta<0$, the fluid tends to sink corresponding to the cold fluid whereas, if $\eta>0$, the fluid tends to lift corresponding to the heat fluid. The term ∇P in Eq.(24) does not include $\nabla P_0=\rho_0\boldsymbol{g}$ in a reference state of hydrostatic equilibrium. Therefore, in terms of Boussinesqe approximation, $\eta\rho$ can be written in the form

$$\eta\rho=\rho-\rho_0=\beta_e\rho_0\Delta T, \quad (25)$$

where β_e is the thermal expansion coefficient. The relation between $\eta\rho$ and the Grashof number Gr is given by

$$\mathrm{Gr}=\frac{g\beta_e\Delta T L^3}{\nu^2}=\frac{g\eta\rho L^3}{\rho_0\nu^2}, \quad (26)$$

where L is the characteristic length. The relation between the perturbation strength parameter η and the Grashof number Gr can be given further

$$\eta=\frac{\mathrm{Gr}\rho_0\nu^2}{\rho g L^3}. \quad (27)$$

Equation (22) multiplied by the internal energy e_k gives

$$\begin{aligned}&e_k\frac{\partial f_{ki}^{\mathrm{eq}}}{2\partial t}+e_k c_{ki\alpha}\frac{\partial f_{ki}^{\mathrm{eq}}}{2\partial r_\alpha}+\left(1-\frac{1}{2\tau}\right)\\&\cdot\left(e_k\frac{\partial f_{ki}^{\mathrm{neq}}}{2\partial t}+e_k c_{ki\alpha}\frac{\partial f_{ki}^{\mathrm{neq}}}{2\partial r_\alpha}\right)\\=&\frac{\boldsymbol{F}_{ki}\cdot\boldsymbol{k}_\alpha e_k}{2\delta t}-\frac{1}{2\tau\delta t}f_{ki}^{\mathrm{neq}}e_k. \quad (28)\end{aligned}$$

Summing Eq.(28) and considering Eqs.(6), (16), (17) and (21), we can obtain the energy equation,

$$\begin{aligned}&\rho\frac{\partial e}{\partial t}+\rho u_\alpha\frac{\partial e}{\partial r_\alpha}-\delta t\left(\tau-\frac{1}{2}\right)\frac{\partial}{\partial r_\alpha}\\&\cdot\left(\frac{2}{D}\rho e\frac{\partial e}{\partial r_\beta}+\rho u_\alpha\frac{\partial e}{\partial t}+\rho u_\alpha u_\beta\frac{\partial e}{\partial r_\beta}\right)=0, \quad (29)\\&\kappa=\frac{2e\delta t}{D}\left(\tau-\frac{1}{2}\right),\end{aligned}$$

where κ is the thermal conductivity. The Prandtl number can be written as

$$\mathrm{Pr}=\frac{\nu}{\kappa}=1. \quad (30)$$

IV. NUMERICAL SIMULATION

To verify the validity of the $D2Q9$ LBE model, we simulate the phenomena of the thermal convection resulting from the differences of temperature in the gravity field for two-dimensional space. It is obvious that differential temperature distribution leads to fluctuations of the fluid density and yields an internal buoyancy force. By taking advantage of the principle of thermal convection, we consider a two-particle system using the $D2Q9$ LBE model in the simulation. One particle is the hot particle f_{ri} corresponding to the hot fluid of high internal energy e_r, and another is the cold particle f_{bi} corresponding to the cold fluid of low internal energy e_b. In terms of criteria (6), the internal energy of fluid can be written as

$$e=\frac{\rho_r e_r+\rho_b e_b}{\rho}. \quad (31)$$

The first numerical experiment is to simulate the thermal convection phenomena in a square cavity, as shown in Fig.6. We take the side length of the square cavity as the characteristic length L. The discrete scales of space and time are

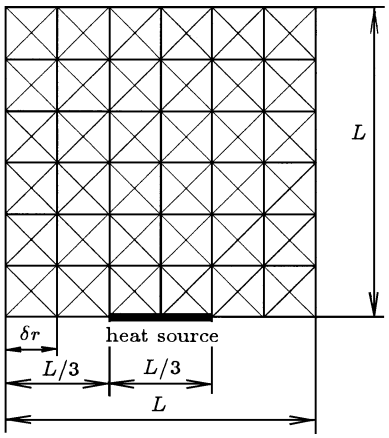


Fig.6. The structural characteristic scales for the thermal flow field.

$$\delta r=\frac{L}{N}, \quad (32)$$

$$\delta t=\frac{\delta r}{c_k}, \quad (33)$$

where N is the discrete number of lattices. Considering Eqs.(27), (32) and (33), the effect of buoyancy force $\boldsymbol{F}_{ki}$ can be written as follows:

$$\boldsymbol{F}_{ri}=+\frac{\mathrm{Gr}\rho_0 c_r(\tau-0.5)^2 f_{ri}}{9\rho N^3 c_{ri\alpha}}\boldsymbol{K}, \quad (34)$$

$$\boldsymbol{F}_{bi}=-\frac{\mathrm{Gr}\rho_0 c_b(\tau-0.5)^2 f_{bi}}{9\rho N^3 c_{bi\alpha}}\boldsymbol{K}, \quad (35)$$

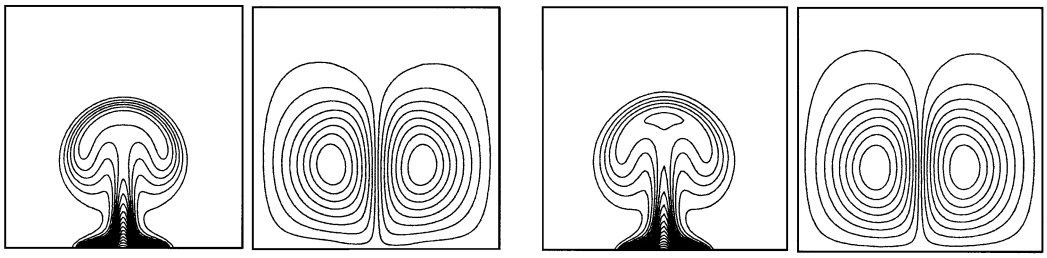
where Eqs.(34) and (35) imply that the hot particles tend to lift and the cold particles tend to sink, as shown in Figs.4 and 5.

The initial condition in the fluid field and on the boundary is for the cold fluid $\rho_b = 1.0$, $e_b = 0.333$, corresponding to the cold particle speed $c_b = 1.0$, and for the hot fluid $\rho_r = 1.0$, $e_r = 1.333$, corresponding to the hot particle speed $c_r = 2.0$. The velocity of fluid flow is taken to be $u_\alpha = 0.0$. The characteristic length and the discrete number of lattices are taken as $L = 1.0$ and $N = 60$, respectively. For the boundary condition we use the thermal flux boundary condition.[7] The so-called thermal flux boundary condition is when a hot particle population collides with the cold boundary wall in which a_c per cent of the hot particles are cooled down and change into cold particles; and, in contrast, a cold particle population collides with the hot boundary wall in which a_h per cent of the cold particles are heated and change into hot particles. For example, in the heating source section of Fig.6, the boundary condition can be expressed by

$$\begin{cases} f_{bi} = f_{bj} - a_\mathrm{h} f_{bj}, \\ f_{ri} = f_{rj} + a_\mathrm{h} f_{bj}, \quad i = 2, 5, 6; \quad j = 4, 7, 8, \end{cases} \tag{36}$$

where the moving direction of particles is given in Fig.4. The cooling coefficient a_c and the heating coefficient a_h have values $0 \le a_\mathrm{c} \le 1$ and $0 \le a_\mathrm{h} \le 1$, respectively. In fact, the thermal flux boundary condition is a progressive bounce-back boundary condition. In this simulation, the heating and cooling coefficients are taken as a_h=0.02 and a_c=0.0. In order to verify the behaviour of the LBE model, we compare the results with the finite-difference solutions of Boussinesqe equations with the same conditions. The numerical results are shown in Fig.7.

Another numerical experiment is to simulate the two-dimensional convection phenomena between two concentric cylinders in which the internal cylinder is the heating source. We take the outer diameter of the internal cylinder as the characteristic length D_i, and the inner diameter of the external cylinder is $2.5D_i$. The initial condition in the flow field and on the boundary is for the cold fluid $\rho_b = 1.0$, $e_b = 0.333$ corresponding to the cold particle speed $c_b = 1.0$, for the hot fluid $\rho_r = 1.0, e_r = 1.333$ corresponding to the hot particle speed $c_r = 2.0$. The velocity of fluid flow is taken to be $u_\alpha = 0.0$. The characteristic length and the discrete number of lattices are taken as $L = 1.0$ and $N = 40$, respectively. The boundary condition is the thermal flux boundary condition, and the heating and cooling coefficients are taken to be $a_\mathrm{h} = 1.0$ and $a_\mathrm{c} = 0.0$, respectively. The numerical results are shown in Fig.8.



(a) **LBM** 15000 steps (b) **FDM** t=6.6

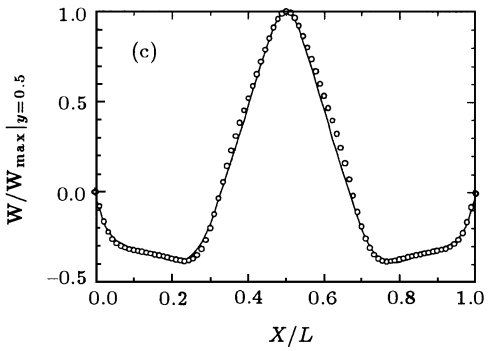


Fig.7. Comparison of temperature field, streamlines and the vertical velocity between LBM and FDM. (c) shows vertical velocity profiles along the horizontal centreline. The solid line represents the results of FDM and the small circles represent those by LBM for Gr=5×10^6, $\tau = 0.505$.

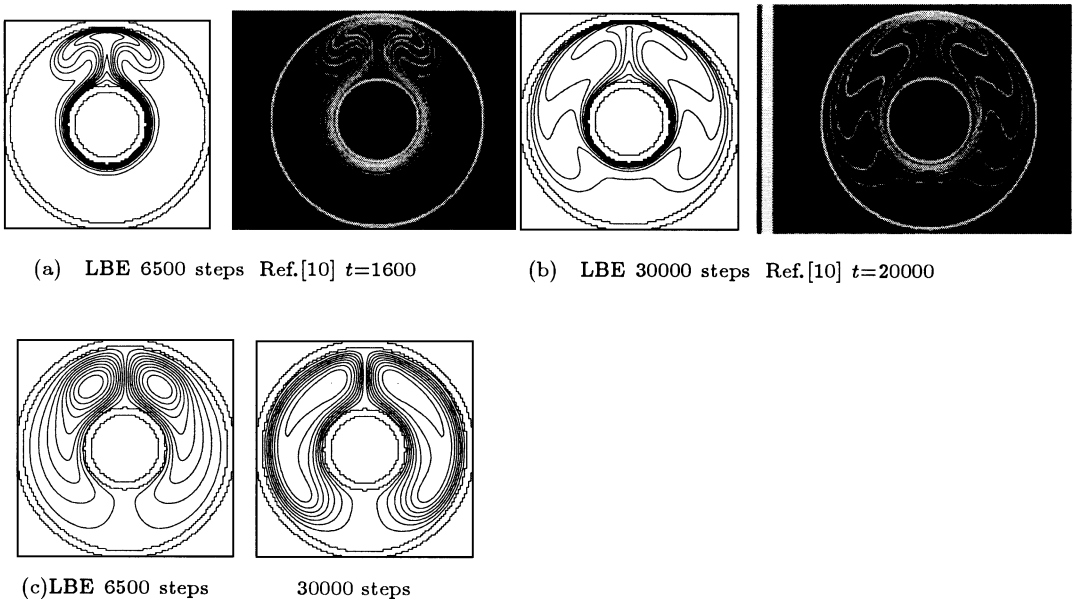


Fig.8. Comparison of the temperature contour between LBM and FEM[9] for Gr=66 000, $\tau = 0.51$. (c) shows the streamlines for LBE.

Both numerical results are qualitatively in good agreement with the conventional numerical methods, as shown in Figs.7 and 8. It is well known among LBE researchers that instability problems arise frequently.[8] To verify the stability, the LBE model can implement the following initial conditions. For example, the fluid density, velocity and internal energy can be taken as $\rho_b = 1.0$, $0 \leq \rho_r \ll 1.0$, $u_\alpha = 0.0$, $e_b = 0.333(c_b = 1.0)$ in the flow field and on the cold boundary. In the heating source, these can be taken as $0 \leq \rho_b \ll 1.0$, $\rho_r = 1.0$, $u_\alpha = 0.0$, $e_b = 1.333(c_r = 1.0)$. If the hot fluid density in the flow field satisfies the condition $0 \leq \rho_r \ll 1.0$, the effect of the buoyancy force can be omitted for the hot particle. The above initial conditions can guarantee the numerical stability of the LBE model.

V. CONCLUSION

In this work, a lattice Boltzmann model has been developed in which the equilibrium distribution functions are third order in u_α. The LBE model strictly satisfies the conservation of mass, momentum and energy, and the internal energy of fluid per unit mass determined by the particle population speed is in agreement with the principle of statistical physics. The effect of the buoyancy force has also been considered in this LBE model, and the numerical results agree very well with the conventional numerical results, showing that the LBE model is both valid in theory and effective in numerical experiment.

ACKNOWLEDGMENT

The authors are indebted to Dr Feng Xue for discussions and helpful suggestions.

References

[1] Frisch U, d'Humières D, Hasslacher B, Lallemand P, Pomeau Y and Rivet J P 1987 *Complex Syst.* **1** 649
[2] Wolfram S 1986 *J. Stat. Phys.* **45** 471
[3] Rothman D H and Zaleskl S 1996 *Lattice-Gas Cellar Automata* (Cambridge University)
[4] McNamara G and Alder B 1993 *Physica* A **194** 218
[5] Alexander F J, Chen S and Sterling D 1993 *Phys. Rev.* **47** 2249
[6] Shan X 1997 *Phys. Rev.* E **55** 2780
[7] Feng S, Tsutahara M, Kataoka T and Takada N 2000 *Mem. Grad. School Sci. Technol. Kobe Univ.* **18** 131
[8] Sterling J D and Chen S J 1996 *Comput. Phys.* **123** 196
[9] Tanahashi T 1991 *Foundations and Applications of Computational Fluid Dynamics* (Tokyo: Tokyo University Press) (in Japanese)
[10] Lu K P 2000 *Chin. Phys.* **9** 81